

Article

Hybrid Forecasting Models Based on the Neural Networks for the Volatility of Bitcoin

Monghwan Seo ¹ and Geonwoo Kim ^{2,*}

¹ Department of Mathematics, Yonsei University, 50 Yonsei-ro Seodaemun-gu, Seoul 03722, Korea; smh3261@naver.com

² School of Liberal Arts, Seoul National University of Science and Technology, Seoul 01811, Korea

* Correspondence: geonwoo@seoultech.ac.kr

Received: 10 June 2020; Accepted: 9 July 2020; Published: 10 July 2020



Abstract: In this paper, we study the volatility forecasts in the Bitcoin market, which has become popular in the global market in recent years. Since the volatility forecasts help trading decisions of traders who want a profit, the volatility forecasting is an important task in the market. For the improvement of the forecasting accuracy of Bitcoin's volatility, we develop the hybrid forecasting models combining the GARCH family models with the machine learning (ML) approach. Specifically, we adopt Artificial Neural Network (ANN) and Higher Order Neural Network (HONN) for the ML approach and construct the hybrid models using the outputs of the GARCH models and several relevant variables as input variables. We carry out many experiments based on the proposed models and compare the forecasting accuracy of the models. In addition, we provide the Model Confidence Set (MCS) test to find statistically the best model. The results show that the hybrid models based on HONN provide more accurate forecasts than the other models.

Keywords: Bitcoin; artificial neural network; higher order neural network; volatility forecasting; hybrid models

1. Introduction and Review of Models

1.1. Introduction

Online transactions over the Internet have depended on trusted financial institutions, which are central players for safe transactions. Nakamoto [1] proposed Bitcoin as a digital currency to provide an easy method to perform online transactions. Bitcoin is a peer-to-peer cryptocurrency system, where Bitcoin transactions occur with no central players. All Bitcoin transactions are verified by the nodes of the peer-to-peer networks and added to the blockchain as the Bitcoin ledger. The information of all historical transactions and all Bitcoin clients is stored in the blockchain. That is, Bitcoin transactions are recorded in the blockchain. The value of Bitcoin is not based on the economic condition in any country and depends on only the supply and demand of the network. Thus, Bitcoin has been utilized widely as a digital currency that can be exchanged for real products or services based on the Bitcoin market value. In fact, there are various digital currencies such as Ethereum, Ripple, Stellar, etc. However, we focus only on Bitcoin because the Bitcoin market capitalization is about 50% of the total estimated digital currency capitalization at present.

As the Bitcoin market has grown over the years, there have been many studies to analyze the Bitcoin market in recent years. Urquhart [2] studied the efficiency of Bitcoin market. In an efficient market, due to the random nature of unpredictable events, variations are random. To find the inefficiency, Urquhart employed a battery of highly powerful tests for randomness and found evidence of inefficiency. The high-frequency multifractal properties of Bitcoin were examined

in [3]. Gajardo et al. [4] analyzed the asymmetric multifractal cross-correlations among stock market indices, commodities and Bitcoin. Yonghong et al. [5] also investigated the time-varying long-term memory in the Bitcoin market. Dyhrberg [6,7] showed that Bitcoin has a clear role in the market for portfolio management. Some researchers studied Bitcoin as an investment vehicle [8–10]. They found out that Bitcoin investment has characteristic features such as high average return and volatility. Although the volatilities of various financial indices have an important impact on the Bitcoin market, the most important factor that affects the high volatility of Bitcoin is the speculative behavior of users. In addition, there was a study on economic analyses of Bitcoin as a currency [11]. According to Iwamura et al. [11] and Yermack [12], Bitcoin may not be suitable as currency since Bitcoin has high volatility. Baur et al. [13] also showed that Bitcoin is used as a speculative investment due to high volatility and large returns. In practice, since the Bitcoin market has high volatility, the study on the volatility of Bitcoin has been very important. We focus on the volatility of Bitcoin in this paper. Specifically, we study the accurate methods for forecasting of Bitcoin volatility.

Many researchers have investigated the analysis and prediction of Bitcoin volatility recently. Baur and Dimpfl [14] analyzed asymmetric volatility effects for Bitcoin. Other studies attempted to show that Bitcoin volatility has some properties such as chaos, randomness, multi-fractality and long-range memory [15,16]. Additionally, there have been many studies on the forecasting of Bitcoin volatility. Balcilar et al. [17] studied the prediction of Bitcoin volatility with a quantile test based on the trading volume. Katsiampa [18] investigated several GARCH family models to find the best model for Bitcoin volatility and found that the AR-CGARCH is the optimal model. Chu et al. [19] provided the best fitting models based on GARCH models for volatilities of cryptocurrencies including Bitcoin. They fit 12 GARCH models to each cryptocurrency and found that IGARCH (1,1) model provides a good fit. Conrad et al. [20] used the GARCH-MIDAS model to improve the prediction of long-term Bitcoin volatility. However, GARCH models have limitations that are hard to capture complex fluctuation and nonlinear correlation of time series data. In order to overcome these limitations, many researchers have proposed the non-parametric forecasting methods based on machine learning approaches such as ANN for better forecasting of Bitcoin volatility [21–23].

Over the past few years, there have been various hybrid models based on ANN to improve the forecasting ability of the time series data. In particular, the hybrid models based on ANN and GARCH models have been proposed to improve forecast accuracy for the time-series data such as market indices, exchange rate, stock volatility, gold price, oil price and metal, etc. [24–30]. These results have shown that the hybrid models have an advantage compared to ANN models. The so-called ANN-GARCH models are the hybrid models that incorporate the GARCH forecasts as the explanatory variables to the ANN models and have been developed consistently by many researchers. For instance, Hajizadeh et al. [31] proposed two ANN-GARCH models to improve the forecasting performance of the S&P 500 index volatility. They used various input variables including financial indicators and the simulated volatility by GARCH models, and the proposed hybrid model with EGARCH model show better accuracy than the traditional GARCH models and ANN models. Kristjanpoller et al. [32] provided the methodology and the application for the volatility forecast of three Latin American stock indexes using a hybrid ANN-GARCH model. Lahmiri and Boukadoum [33] presented an ensemble system based on a hybrid EGARCH-ANN model which is trained with a different distributional assumption. In addition, Seo et al. [34] constructed the hybrid ANN-GARCH model with Google domestic trend and various activation functions for better forecasting accuracy of S&P 500 index volatility. In this paper, we also employ the ANN-GARCH models for accurate forecasting of the realized volatility of Bitcoin. Specifically, we develop ANN-GARCH models with HONN and Google trends (GT) data and compare the proposed models to find the best fitting model for Bitcoin volatility.

The contribution of this work is to find the optimal hybrid model for forecasting Bitcoin's volatility. To present our result, this paper is structured as follows. In the next subsection, we review the models used in this paper. In Section 2, we describe the data used for the proposed hybrid models. In Section 3,

we construct efficient hybrid models and provide the results of the experiments by the proposed models. In Section 4, we present the concluding remarks.

1.2. Review of Models

In this section, we introduce GARCH family models used to construct our hybrid models. More specifically, we review the GARCH model, EGARCH model and GJR-GARCH model. The forecasts by GARCH family models are used as the explanatory variables to ANN. We also review ANN model and HONN model with various activation functions used in this paper.

1.2.1. GARCH Model

The ARCH model proposed by Engle [35] was the first model with the conditional distribution to describe the fat tail characteristics or the volatility clustering properties of time series. However, the ARCH model has computational problems when a large number of parameters are needed for a high order model. To solve these problems, Bollerslev [36] proposed the GARCH model, which is one of the most popular models for forecasting the volatility of time series. Since the GARCH models include the conditional variance terms as well as the squared residual terms, the models can predict the volatility well by using a sum of weighted products of the predicted variance from the past.

The GARCH (p, q) model is defined as the follows.

$$y_t^2 = w + \sum_{i=1}^q \alpha_i \varepsilon_{t-i}^2 + \sum_{i=1}^p \beta_i y_{t-i}^2, \quad (1)$$

where $\varepsilon_t = y_t Z_t$, $\{Z_t\}$ is a sequence of independent and identically distributed random variables with zero mean and unit variance, $\{\varepsilon_t\}$ is a sequence of the error terms, the positive parameters α_i and β_i satisfy the condition $\sum_{i=1}^q \alpha_i + \sum_{i=1}^p \beta_i < 1$ for the stability of the GARCH model. This condition ensures that the conditional variance y_t has nonnegative values and finite expected value. Here, w , α_i and β_i are the estimated parameters by using maximum likelihood estimation.

1.2.2. EGARCH Model

The exponential GARCH (EGARCH) model proposed by Nelson [37] allows negative parameters unlike the GARCH model. That is, the parameters of the model have no restrictions to ensure the non-negativity of the volatility. This model can describe the volatility leverage effect which reflects the asymmetric impacts and captures asymmetric behavior of the time series.

The EGARCH (p, q) model is defined as follows.

$$\log y_t^2 = w + \sum_{i=1}^q \alpha_i \left[\frac{|\varepsilon_{t-i}|}{y_{t-i}} - \sqrt{\frac{2}{\pi}} + \gamma \frac{\varepsilon_{t-i}}{y_{t-i}} \right] + \sum_{i=1}^p \beta_i \log y_{t-i}^2, \quad (2)$$

where α_i with no restrictions captures the volatility clustering effect, β_i measures the persistence in conditional volatility irrespective of the events in the market and γ measures the asymmetric leverage coefficient to describe the leverage effect of volatility. α_i , β_i and γ are parameters to be estimated.

1.2.3. GJR-GARCH Model

The GJR-GARCH model proposed by Glosten et al. [38] is one of nonlinear GARCH family models to allow for asymmetry effects by integrating a dichotomous variable into the GARCH model. This model allows the larger impact of negative shocks to have a more distinct impact on volatility than a positive impact. The model also presented improved forecasting ability [39].

The conditional variance of GJR-GARCH (p, q) model is defined as follows.

$$y_t^2 = w + \sum_{i=1}^q \left[\alpha_i + \gamma_i \mathbf{1}_{\{\varepsilon_{t-i} < 0\}} \right] \varepsilon_{t-i}^2 + \sum_{i=1}^p \beta_i y_{t-i}^2 \tag{3}$$

where

$$\mathbf{1}_{\{\cdot\}} = \begin{cases} 1, & \varepsilon_{t-i} < 0, \\ 0, & \varepsilon_{t-i} \geq 0, \end{cases}$$

and

$$w \geq 0, p \geq 0, q \geq 0, \alpha_i \geq 0, \beta_i \geq 0, \alpha_i + \gamma_i \geq 0 \text{ and } \sum_{i=1}^p \alpha_i + \sum_{i=1}^q \beta_i + \frac{1}{2} \sum_{i=1}^q \gamma_i < 1.$$

where α_i and β_i are similar to the coefficients in the EGARCH model, and γ_i means the asymmetric leverage coefficient. The parameters w, α_i, β_i and γ_i are estimated by the maximum likelihood approach.

1.2.4. Artificial Neural Network (ANN)

ANN is one of the nonparametric nonlinear models which are used widely to overcome the limitations of the linear models in machine learning. ANN is constructed appropriately based on the characteristics extracted from the real data and has no hypothesis about the underlying model. ANN also has at least three layers (input layer, hidden layer, output layer). ANN with single hidden layer used for forecasting is illustrated in Figure 1.

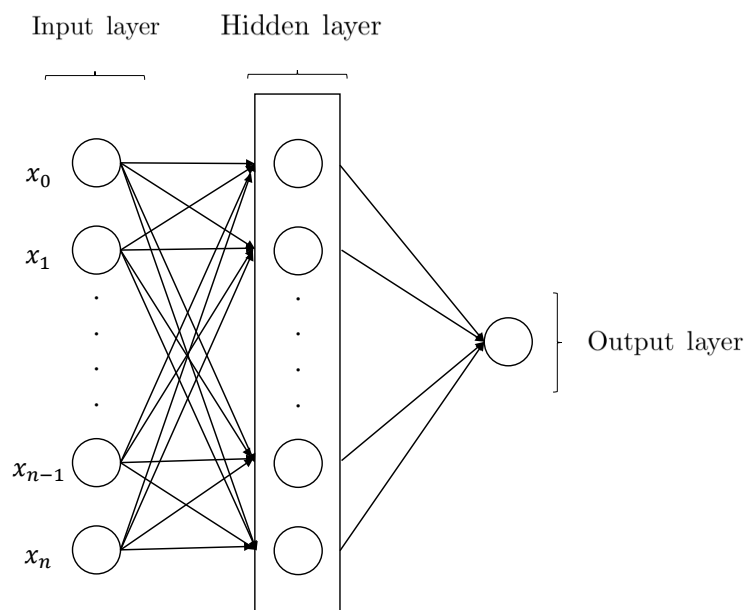


Figure 1. The structure of Artificial Neural Network (ANN).

The output result from input layer and hidden layer is generally as follows.

$$\text{output} = f \left(\sum_{i=0}^n x_i w_i \right), \tag{4}$$

where x_i and w_i represent the set of input data from node i and the weight associated with the connection to the node i , and f is one of the activation functions. The activation functions used in this paper are presented in Table 1. The sigmoid function shows high sensitivity to small changes in input variables. This property provides a good classifier. The hyperbolic tangent function (Tanh) has an advantage over the sigmoid function. Since the derivative of the function is steeper, it will

have faster learning and grading. In addition, it is well known that the Rectified Linear Unit (ReLU) is a good estimator and show very efficient calculation when all neurons are activated in the same manner. Exponential Linear Unit (ELU) provides fast learning because ELU shrinks the difference between the unit natural gradient and the normal gradient.

Table 1. Activation functions used in this paper.

| Name | Activation Function |
|-------------------------------|--|
| Sigmoid | $f(x) = \frac{1}{1+e^{-x}}$ |
| Hyperbolic Tangent (Tanh) | $f(x) = \frac{e^x - e^{-x}}{e^x + e^{-x}}$ |
| Rectified Linear Unit (ReLU) | $f(x) = \begin{cases} 0 & \text{for } x < 0 \\ x & \text{for } x \geq 0 \end{cases}$ |
| Exponential Linear Unit (ELU) | $f(x) = \begin{cases} \alpha(e^x - 1) & \text{for } x < 0 \\ x & \text{for } x \geq 0 \end{cases}$ |

The main work of ANN is to find the optimal weights for better performance using the activation functions. We use the back-propagation method to obtain the weights. We also carry out many experiments with four activation functions to find the best forecasting model.

1.2.5. Higher Order Neural Network (HONN)

HONN proposed by Giles and Maxwell [40] has been widely used to simulate the higher-order nonlinear inputs and to provide some basis for the simulations as ‘open box’ [41]. Because first-order networks do not take advantage of meaningful relationships between the input variables, the networks need a lot of training passes with a large training set. To improve this disadvantage, HONN has been developed. In general, with the selection of good input variables, it is known that HONN provides better forecasting performance than the classic ANN.

In Equation (4), the independent variable is presented as the linear combination. Specifically, the variable is expressed by multiplying each input variable (x_i) by a weight (w_i) and adding the results. We can easily make out the higher-order terms of the inputs from the first-order terms. Here, we consider the second order HONN to improve the volatility forecasting. Let us define the input vector \vec{x} and the weight vector \vec{w} by

$$\vec{x} = [x_0, x_1, \dots, x_n] \text{ and } \vec{w} = [w_0, w_1, \dots, w_n],$$

respectively. Then the input vector \vec{x}_h and the weight vector \vec{w}_h in HONN are given by

$$\vec{x}_h = [x_0, x_1, \dots, x_n, x_0^2, x_0x_1, x_0x_2, \dots, x_{n-1}x_n, x_n^2] \text{ and } \vec{w}_h = [w_0, w_1, \dots, w_n, w_{00}, w_{01}, w_{02}, \dots, w_{n-1n}, w_{nn}],$$

respectively. From these vectors, the output with the activation functions f can be calculated as follows.

$$\text{output} = f(\vec{w}_h \cdot \vec{x}_h) = f\left(\sum_{i=0}^n w_i x_i + \sum_{i=0}^n \sum_{j=i}^n w_{ij} x_i x_j\right). \tag{5}$$

The structure of a second-order HONN used in this paper is illustrated in Figure 2. We construct the hybrid models based on this second-order HONN for the accurate forecasting.

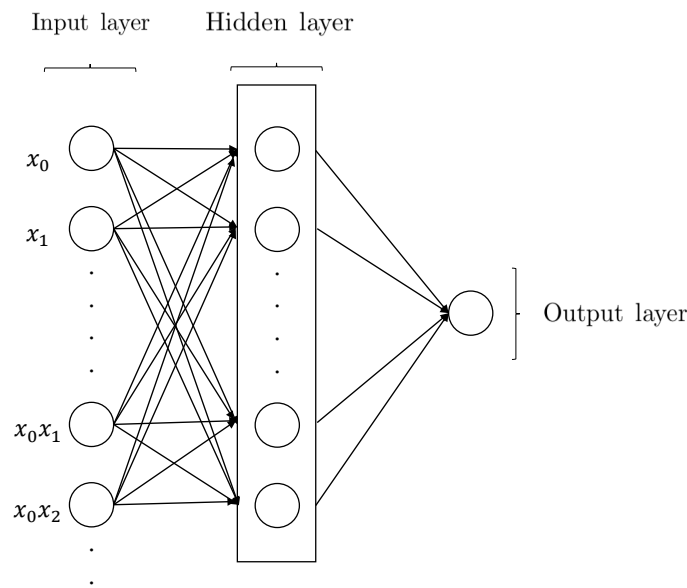


Figure 2. The structure of Higher Order Neural Network (HONN).

2. Material and Methods

The time series data analyzed in this paper were the daily historical prices of Bitcoin over the period between 1 January 2012 and 30 November 2019. The data were downloaded from the website (<https://bitcoincharts.com/>). To define the volatility of Bitcoin price, the closing prices p_t at time t are transformed into log return $r_t = \log p_t - \log p_{t-1}$. The realized volatility of Bitcoin was computed as the variance of r_t , and the realized volatilities in a 5-day window as weekly volatilities are used to analyze the volatility of Bitcoin in this paper. Then, the realized volatility (RV_t) of Bitcoin at time t is computed as

$$RV_t = \frac{1}{5} \sum_{i=t+1}^{t+5} (r_i - \bar{r}_t)^2,$$

where \bar{r}_t is mean of r_t during 5 days after time t .

In order to improve the accuracy of the volatility forecast, the selection of the input data which influence on the volatility of Bitcoin is very important. In this paper, we consider the GT data and VIX data as the explanatory variables. GT is the data that presents the popularity of search queries related to various sectors in Google. In fact, GT data has been used as explanatory variables in the ANN to forecast of the financial time series by many researchers [34,42–44]. We used ‘Bitcoin’ GT data as the input variable, which is a good measure to describe the Bitcoin market [45]. VIX index introduced the Chicago Board Options Exchange (CBOE) in 2004 extrapolates the future volatility from the liquid options written on the S&P 500 and is calculated as the square root of the risk-neutral expectation of the 30 days variance of the S&P 500 return which is estimated by the forward option price expiring in 30 days. From the previous works [46,47], we can find the significant relationship between the VIX index and Bitcoin. Thus, we choose the VIX index as the input data to the ANN-based on the researches. Specifically, 5-days moving averages of VIX index and GT data are used as the input data. In Figure 3, the time series of log return r_t of Bitcoin price are displayed. Figures 4 and 5 illustrate the realized volatility of bitcoin price and VIX index, respectively.

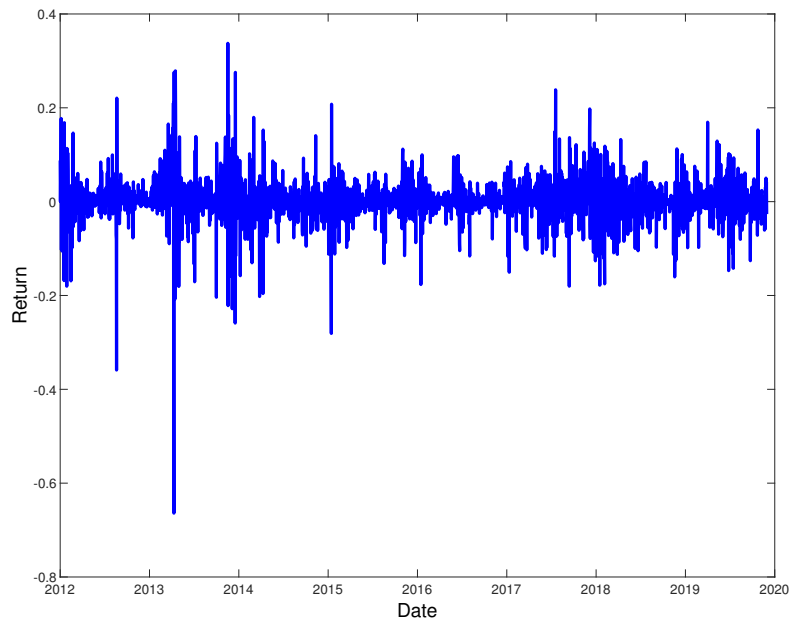


Figure 3. Log return r_t of Bitcoin price from 1 January 2012 to 30 November 2019.

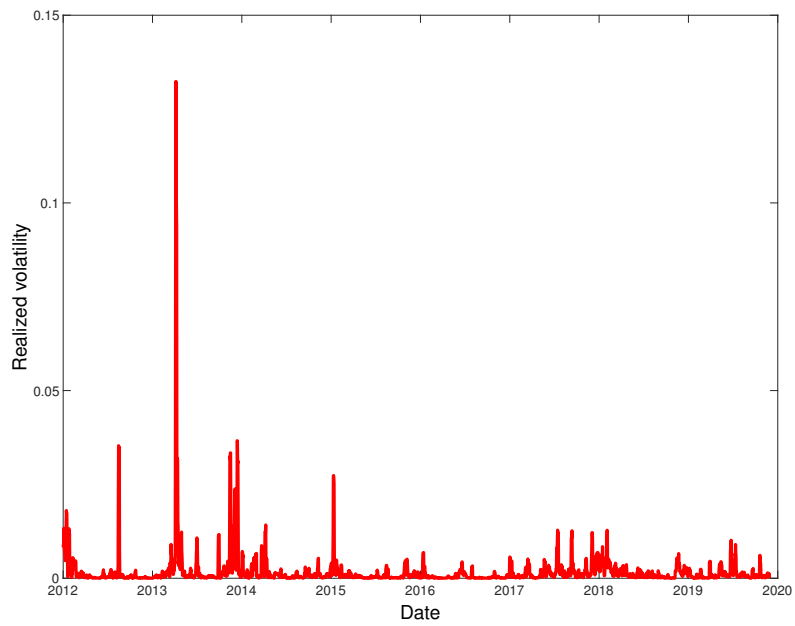


Figure 4. Realized volatility RV_t of r_t from 1 January 2012 to 30 November 2019.

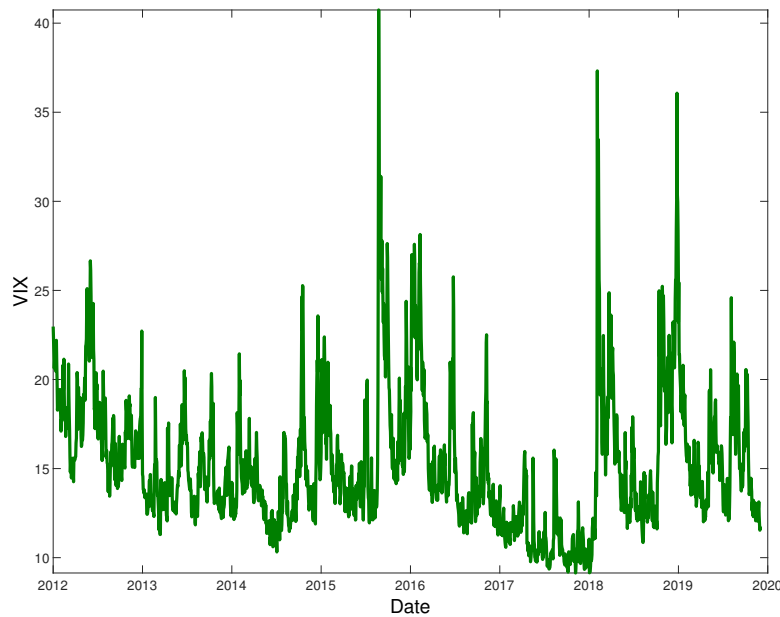


Figure 5. VIX index from 1 January 2012 to 30 November 2019.

In order to construct a more accurate model for forecasting of Bitcoin volatility, we use the 1-day lagged weekly volatility (LV_t) as the endogenous variable and the outputs of GARCH family models as the exogenous variables. In other words, LV_t and GARCH family outputs are used as the input variables to improve the forecasting ability of the hybrid model. Here, the outputs of the GARCH models introduced in the previous section are used, and LV_t is calculated by

$$LV_t = \frac{1}{5} \sum_{i=t-1}^{t-5} (r_i - \bar{r}_t)^2. \tag{6}$$

Note that days in windows of LV_t have no intersection with 5 days in windows of RV_t . LV_t is displayed in Figure 6. In this study, 80% of the data set (in-sample: 2012.01.01–2018.04.30) are used for training, and 20% (out-of-sample: 2018.05.01–2019.11.30) of the data set are used for testing. All experiments are implemented using Python 3. Additionally, we utilize three measures to compare the performance of the proposed models. These measures are the mean absolute error (MAE), the root mean square error (RMSE) and the mean absolute percentage error (MAPE) and as follows.

$$\begin{aligned} MAE &= \frac{1}{n} \sum_t |\hat{\sigma}_t - RV_t|, \\ RMSE &= \left(\frac{1}{n} \sum_t (\hat{\sigma}_t - RV_t)^2 \right)^{1/2}, \\ MAPE &= \frac{1}{n} \sum_t \left| \frac{\hat{\sigma}_t - RV_t}{RV_t} \right|, \end{aligned}$$

where $\hat{\sigma}_t$ is the predicted volatility of Bitcoin and n is the number of the predicted data. Obviously, the lower values of the measures, the better accuracy of the model. For more details, see [48].

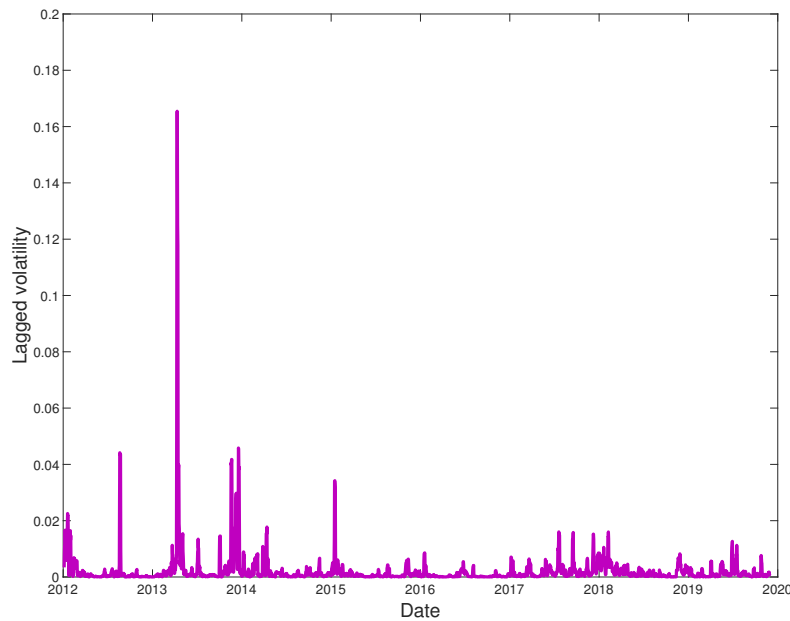


Figure 6. Lagged volatility LV_t of r_t from 1 January 2012 to 30 November 2019.

3. Hybrid Models and Results

In this paper, we propose several hybrid models based on GARCH family models, ANN and HONN to find a more accurate model for forecasting of Bitcoin volatility. Specifically, the hybrid models are constructed with the ANN by using the selected GARCH models and the selected explanatory variables. The models are implemented by the ANN with a single hidden layer and various neurons using the back-propagation method and classified according to whether including the explanatory variables or not. The proposed models are used for 1-day ahead forecast of weekly realized volatility, and then the best model is determined by comparing the results.

We compare the proposed models to find the best volatility forecasting model in the bitcoin market. We first forecast the volatility of Bitcoin price using the classic GARCH family models. Concretely, we use GARCH, EGARCH and GJR-GARCH model among the GARCH family models and the (p, q) parameters ranging from (1,1) to (3,3). In order to find the optimal GARCH model for the hybrid model, we provide AIC and BIC values in Table 2 and three measures to compare the performances of the models for forecasting volatilities in Table 3. According to the results in Table 2 and AIC and BIC criteria, EGARCH(3,3) model is the best model. On the other hand, according to the results in Table 3, we can see that the GJR-GARCH(1,1) model performs the best among the introduced GARCH family models.

Table 2. GARCH models.

| Models | (p, q) | AIC | BIC |
|-----------|----------|----------|----------|
| GARCH | (1,1) | −7593.56 | −7570.83 |
| GARCH | (2,2) | −7633.38 | −7599.30 |
| GARCH | (3,3) | −7630.73 | −7585.28 |
| GJR-GARCH | (1,1) | −7589.75 | −7561.34 |
| GJR-GARCH | (2,2) | −7577.91 | −7538.14 |
| GJR-GARCH | (3,3) | −7558.42 | −7507.29 |
| EGARCH | (1,1) | −7646.91 | −7618.51 |
| EGARCH | (2,2) | −7665.96 | −7626.19 |
| EGARCH | (3,3) | −7687.68 | −7636.55 |

Table 3. GARCH models performance.

| Models | (<i>p, q</i>) | MAE | RMSE | MAPE |
|-----------|-----------------|-------------|-------------|-------------|
| GARCH | (1,1) | 0.01820086 | 0.022997082 | 60.71728437 |
| GARCH | (2,2) | 0.018615039 | 0.023244302 | 62.97792289 |
| GARCH | (3,3) | 0.031275112 | 0.274933282 | 104.4275052 |
| GJR-GARCH | (1,1) | 0.018100989 | 0.022782066 | 59.57816469 |
| GJR-GARCH | (2,2) | 0.018273329 | 0.022976453 | 61.3172729 |
| GJR-GARCH | (3,3) | 0.018353907 | 0.023128309 | 61.44172661 |
| EGARCH | (1,1) | 0.021923047 | 0.025916869 | 80.21691954 |
| EGARCH | (2,2) | 0.021758949 | 0.025850653 | 79.23566863 |
| EGARCH | (3,3) | 0.022439612 | 0.026596278 | 81.70952727 |

Other models except for the classic GARCH models are based upon the ANN approach or the HONN approach. In other words, the models are constructed by using the selected input variables to ANN or HONN. Similar to [31,34], we propose the ANN-GARCH models for the forecasting of the Bitcoin volatility using the outputs of the GARCH family models. Specifically, we define the GT-GARCH model and GT-VIX-GARCH model according to the input variables. The input variables of the models are in Table 4. In order to find the optimal number of nodes in the hidden layer and the activation function for the models, we carry out the experiments using the Adam optimizer method [49] to update the network weights. The results are indicated with four activation functions in Tables 5 and 6. As shown in Tables 5 and 6, two measures (MAE, RMSE) show that the GT-GARCH model is better than the GT-VIX-GARCH model, and one measure (MAPE) shows a different result. From these results, we can not find a significant performance difference between the GT-VIX-GARCH model and the GT-GARCH model. That is, we conclude that two models may have a similar predictive ability. To improve the accuracy of the model, we adopt the HONN approach. Specifically, we propose three types of hybrid models (GT-H model, GT-VIX-H model, GT-VIX-GARCH-H model) based on the HONN.

Tables 7–9 are presented the results of the models based on the HONN. To examine well the proposed models based on the HONN, we present a summary of the input variables of each model in Table 10. In Table 10, ‘*LV_t*’ is in Equation (6), ‘GT’ means Google trends data, ‘VIX’ means VIX index data, ‘GJR-GARCH(1,1)’ means forecast by GJR-GARCH(1,1) and ‘EGARCH(3,3)’ means forecast by EGARCH(3,3). Tables 7 and 8 present the results of the HONN model without the outputs of GARCH models as shown in Table 10. We can see that MAE and MAPE in Tables 7 and 8 increase in all cases as compared to the values in Tables 5 and 6. That is, GT-H model and GT-VIX-H model do not show better performance compared to the models based on the ANN. To improve the model, we adopt the HONN model with the outputs of GARCH family models. Among the introduced GARCH models, we chose GJR-GARCH(1,1) and EGARCH(3,3) from the results in Tables 2 and 3. By using the outputs of GJR-GARCH(1,1) and EGARCH(3,3) as input variables in the HONN, we finally construct and propose a new type of hybrid model (GT-VIX-GARCH-H model) for better forecasting of Bitcoin volatility.

Table 4. Input variables of models.

| Models | Selected Input Variables |
|--------------------|---|
| GT-GARCH model | {GARCH(1,1), GARCH(2,2), GARCH(3,3), GJR-GARCH(1,1), GJR-GARCH(2,2), GJR-GARCH(3,3), EGARCH(1,1), EGARCH(2,2), EGARCH(3,3), GT, <i>LV_t</i> } |
| GT-VIX-GARCH model | {GARCH(1,1), GARCH(2,2), GARCH(3,3), GJR-GARCH(1,1), GJR-GARCH(2,2), GJR-GARCH(3,3), EGARCH(1,1), EGARCH(2,2), EGARCH(3,3), GT, <i>LV_t</i> , VIX } |

Table 5. GT-GARCH model performance.

| Model | Activation Function | Nodes | MAE | RMSE | MAPE |
|----------|---------------------|-------------|-------------|-------------|-------------|
| GT-GARCH | Relu | 10 | 0.016455061 | 0.0228628 | 44.03939302 |
| | | 20 | 0.016455761 | 0.02286762 | 44.01794052 |
| | | 30 | 0.016456899 | 0.022870071 | 44.01377941 |
| | | 40 | 0.016457765 | 0.02287134 | 44.01490369 |
| | | 50 | 0.016456698 | 0.022868367 | 44.01481934 |
| | Tanh | 10 | 0.01645589 | 0.022866914 | 44.02158481 |
| | | 20 | 0.016456046 | 0.022867024 | 44.02205182 |
| | | 30 | 0.016457015 | 0.022869247 | 44.01766755 |
| | | 40 | 0.016457969 | 0.022870135 | 44.0273439 |
| | | 50 | 0.016457073 | 0.022869712 | 44.01422672 |
| | Elu | 10 | 0.016456301 | 0.022867778 | 44.01894413 |
| | | 20 | 0.016451684 | 0.02284573 | 44.10871 |
| | | 30 | 0.016456961 | 0.022866742 | 44.03292253 |
| | | 40 | 0.016455294 | 0.022864722 | 44.02362704 |
| | | 50 | 0.016456115 | 0.022866339 | 44.0296898 |
| Sigmoid | 10 | 0.016456811 | 0.02286878 | 44.02080023 | |
| | 20 | 0.016457144 | 0.022869732 | 44.01885011 | |
| | 30 | 0.016456885 | 0.022867327 | 44.02887424 | |
| | 40 | 0.016456888 | 0.022870528 | 44.01028107 | |
| | 50 | 0.016457102 | 0.022868327 | 44.02443017 | |

Table 6. GT-VIX-GARCH model performance.

| Model | Activation Function | Nodes | MAE | RMSE | MAPE |
|--------------|---------------------|-------------|-------------|-------------|-------------|
| GT-VIX-GARCH | Relu | 10 | 0.016464618 | 0.022961953 | 43.6754142 |
| | | 20 | 0.016463169 | 0.022961503 | 43.66309023 |
| | | 30 | 0.016464239 | 0.022963376 | 43.66271481 |
| | | 40 | 0.016464096 | 0.022965466 | 43.65610286 |
| | | 50 | 0.016468159 | 0.022966994 | 43.68492065 |
| | Tanh | 10 | 0.016465239 | 0.022964124 | 43.67126798 |
| | | 20 | 0.016463913 | 0.022960066 | 43.67926114 |
| | | 30 | 0.016464939 | 0.022962888 | 43.67179649 |
| | | 40 | 0.01646529 | 0.022962936 | 43.68079538 |
| | | 50 | 0.016463781 | 0.022958457 | 43.68308928 |
| | Elu | 10 | 0.016464796 | 0.022964955 | 43.66256389 |
| | | 20 | 0.016465883 | 0.02296502 | 43.67128545 |
| | | 30 | 0.016464635 | 0.022962084 | 43.67544449 |
| | | 40 | 0.016466452 | 0.022966505 | 43.66998111 |
| | | 50 | 0.016462585 | 0.022957731 | 43.67119374 |
| Sigmoid | 10 | 0.01646477 | 0.022963578 | 43.67003712 | |
| | 20 | 0.016461495 | 0.022957864 | 43.67131767 | |
| | 30 | 0.016464624 | 0.022961432 | 43.67831534 | |
| | 40 | 0.016464975 | 0.022965387 | 43.66149144 | |
| | 50 | 0.01647861 | 0.02302727 | 43.4274305 | |

Table 7. GT-H model performance.

| Model | Activation Function | Nodes | MAE | RMSE | MAPE |
|-------|---------------------|-------|-------------|-------------|-------------|
| GT-H | Relu | 10 | 0.016941584 | 0.022027929 | 52.70636488 |
| | | 20 | 0.016941599 | 0.02202816 | 52.70680583 |
| | | 30 | 0.016941163 | 0.022027678 | 52.70298093 |
| | | 40 | 0.016940914 | 0.022027074 | 52.70274993 |
| | | 50 | 0.016941279 | 0.022027853 | 52.70347102 |
| | Tanh | 10 | 0.016941714 | 0.022027935 | 52.70708064 |
| | | 20 | 0.016942079 | 0.022028228 | 52.70821739 |
| | | 30 | 0.016941977 | 0.022028122 | 52.70722389 |
| | | 40 | 0.016941485 | 0.022028033 | 52.70475844 |
| | | 50 | 0.016940999 | 0.022027369 | 52.70261778 |
| | Elu | 10 | 0.01694181 | 0.022028066 | 52.70750404 |
| | | 20 | 0.016941503 | 0.022027574 | 52.70587155 |
| | | 30 | 0.016942019 | 0.022027821 | 52.7097488 |
| | | 40 | 0.01694203 | 0.022027968 | 52.70826475 |
| | | 50 | 0.01694185 | 0.022027961 | 52.71021157 |
| | Sigmoid | 10 | 0.016941511 | 0.022027945 | 52.70543218 |
| | | 20 | 0.016941295 | 0.022027628 | 52.70568077 |
| | | 30 | 0.016941514 | 0.022028015 | 52.70581447 |
| | | 40 | 0.016942199 | 0.022028407 | 52.70889483 |
| | | 50 | 0.016941966 | 0.022027852 | 52.70746498 |

Table 8. GT-VIX-H model performance.

| Model | Activation Function | Nodes | MAE | RMSE | MAPE |
|----------|---------------------|-------|-------------|-------------|-------------|
| GT-VIX-H | Relu | 10 | 0.016745304 | 0.022489019 | 48.02497968 |
| | | 20 | 0.01674541 | 0.02248914 | 48.0246867 |
| | | 30 | 0.016746443 | 0.022489882 | 48.02759455 |
| | | 40 | 0.016745041 | 0.022488647 | 48.02404413 |
| | | 50 | 0.016748236 | 0.022522086 | 47.82463374 |
| | Tanh | 10 | 0.016745657 | 0.022489571 | 48.02533742 |
| | | 20 | 0.016745787 | 0.02248942 | 48.02683015 |
| | | 30 | 0.016745458 | 0.02248931 | 48.02374776 |
| | | 40 | 0.016744942 | 0.022489028 | 48.0238152 |
| | | 50 | 0.01674544 | 0.022489515 | 48.02256555 |
| | Elu | 10 | 0.01674516 | 0.02248885 | 48.02508728 |
| | | 20 | 0.016745349 | 0.022488898 | 48.02401028 |
| | | 30 | 0.016745336 | 0.022489 | 48.02517194 |
| | | 40 | 0.016745663 | 0.022488933 | 48.02556819 |
| | | 50 | 0.016745491 | 0.022489525 | 48.02760086 |
| | Sigmoid | 10 | 0.016745208 | 0.022489047 | 48.02402778 |
| | | 20 | 0.016745744 | 0.022489067 | 48.02780298 |
| | | 30 | 0.0167453 | 0.022489284 | 48.0246795 |
| | | 40 | 0.016745533 | 0.022488691 | 48.02600782 |
| | | 50 | 0.016745073 | 0.022489534 | 48.02441867 |

Table 9. GT-VIX-GARCH-H model performance.

| Model | Activation Function | Nodes | MAE | RMSE | MAPE |
|----------------|---------------------|-------------|-------------|-------------|--------------|
| GT-VIX-GARCH-H | Relu | 10 | 0.016099377 | 0.022304876 | 41.97126277 |
| | | 20 | 0.016101827 | 0.02228648 | 42.07658833 |
| | | 30 | 0.016095555 | 0.022284853 | 42.03342476 |
| | | 40 | 0.016109686 | 0.022277813 | 42.13001676 |
| | | 50 | 0.016097934 | 0.02228606 | 42.05669279 |
| | Tanh | 10 | 0.016098348 | 0.022302633 | 41.964812188 |
| | | 20 | 0.01609808 | 0.022231812 | 42.38508374 |
| | | 30 | 0.016094577 | 0.022298402 | 42.01919185 |
| | | 40 | 0.016098404 | 0.022302775 | 42.04282541 |
| | | 50 | 0.016096921 | 0.022285756 | 42.04785915 |
| | Elu | 10 | 0.016108832 | 0.02236164 | 41.71558473 |
| | | 20 | 0.016100976 | 0.022290669 | 42.06674165 |
| | | 30 | 0.016098687 | 0.022285274 | 42.06192355 |
| | | 40 | 0.016101002 | 0.022291082 | 42.06727282 |
| | | 50 | 0.016105162 | 0.022295976 | 42.088699 |
| Sigmoid | 10 | 0.016099661 | 0.022292957 | 42.06001306 | |
| | 20 | 0.016099905 | 0.022281962 | 42.06856524 | |
| | 30 | 0.016100028 | 0.022278299 | 42.07671847 | |
| | 40 | 0.016105448 | 0.022285267 | 42.1902812 | |
| | 50 | 0.016096398 | 0.02229977 | 42.03760228 | |

Table 10. Input variables of models.

| Models | Input Variables | | | | |
|----------------------|-----------------|--------------|---------------|--------------------------|-----------------------|
| | $LV_t (x_0)$ | GT (x_1) | VIX (x_2) | GJR-GARCH(1,1) (x_3) | EGARCH(3,3) (x_4) |
| GT-H model | O | O | X | X | X |
| GT-VIX-H model | O | O | O | X | X |
| GT-VIX-GARCH-H model | O | O | O | O | O |

Table 9 shows the results of three performance measures obtained by the GT-VIX-GARCH-H model. We can see the improvement in forecasting accuracy in Table 9. The results in Table 9 show that the hybrid models with selected GARCH models based on the HONN model for volatility forecasting of Bitcoin reduce the performance measures (MAE, RMSE, MAPE). That is, in all cases, the measures decrease compared to the measures of the other models. More specifically, compared to the GJR-GARCH(1,1) forecast, MAE is reduced by 11 %, MAPE is reduced by 30 %. Furthermore, we analyze the robustness of our results to determine whether the proposed models are statistically significant. For the analysis, we apply the MCS test [50] to GT-VIX-GARCH-H models. The detailed results of the MCS test, which can be interpreted as a level of confidence for the forecasts, are presented in Table 11. According to the results in Table 11, we can find that the GT-VIX-GARCH-H model with the Relu function and 30 nodes, which has the lowest MAE, is the best model for forecasting of Bitcoin volatility.

Table 11. Model confidence set.

| Loss Function Ranking | Model | Activation Function | Nodes | MAE | MCS |
|-----------------------|----------------|---------------------|-------|-------------|-------|
| 1 | GT-VIX-GARCH-H | Relu | 30 | 0.016095555 | 1.000 |
| 2 | GT-VIX-GARCH-H | Tanh | 20 | 0.01609808 | 0.991 |
| 3 | GT-VIX-GARCH-H | Tanh | 30 | 0.016094577 | 0.991 |
| 4 | GT-VIX-GARCH-H | Relu | 50 | 0.016097934 | 0.991 |
| 5 | GT-VIX-GARCH-H | Tanh | 40 | 0.016098404 | 0.991 |

4. Concluding Remarks

We develop the models based on the neural networks for forecasting volatility of Bitcoin price in this paper. Specifically, we propose several hybrid models to improve the forecasting and conduct more than 10,000 experiments to find the optimized model. We investigate as follows. Firstly, we construct the ANN-GARCH models with 1-day lagged volatility, Google Trends, VIX and outputs of GARCH models based on the previous works. Secondly, we propose the new hybrid models which incorporate the outputs of GARCH models as input to HONN model. HONN model, which use the linear combinations of the variables as the input variables, is efficient and performs generally better than the classic ANN mode when the number of good input variables for the ANN model is small. In fact, most of the proposed hybrid models show good performances with no statistical difference, but we focus on finding the best forecasting model for Bitcoin's volatility.

In order to find the best model among the proposed models, we carry out many experiments changing the activation functions and the number of nodes. We also adopt three performance measures to compare the forecasting accuracy of the proposed models. Consequently, the hybrid models based on the HONN model which can capture higher-order correlations in input variables show the improved performance for forecasting of Bitcoin volatility. Compared to the best GARCH model, the best GT-VIX-GARCH-H model improves by 11%, 2.2% and 30% for MAE, RMSE and MAPE, respectively. In addition, compared to the best ANN-GARCH model, the best GT-VIX-GARCH-H model improves by 2.2%, 2.5% and 3.9% for MAE, RMSE and MAPE, respectively. In other words, these results show that the hybrid models based on the HONN model provide more accurate forecasting results and are appropriate for forecasting of volatility in the Bitcoin market.

Author Contributions: G.K. designed the experiments; M.S. collected and analyzed the data; M.S. and G.K. contributed analysis tools; M.S. and G.K. wrote the paper. All authors have read and agreed to the published version of the manuscript.

Funding: This work is supported by the National Research Foundation of Korea grant funded by the Korea government (No. NRF-2017R1E1A1A03070886).

Conflicts of Interest: The authors declare no conflict of interest.

References

1. Nakamoto, S. *Bitcoin: A Peer-to-Peer Electronic Cash System*; ReadLiberty.Org: Chicago, IL, USA, 2008.
2. Urquhart, A. The inefficiency of Bitcoin. *Econ. Lett.* **2016**, *148*, 80–82. [[CrossRef](#)]
3. Stavroyiannis, S.; Babalos, V.; Bekiros, S.; Lahmiri, S.; Uddin, G.S. The high frequency multifractal properties of Bitcoin. *Physica A* **2019**, *520*, 62–71. [[CrossRef](#)]
4. Gajardo, G.; Kristjanpoller, W.D.; Minutolo, M. Does bitcoin exhibit the same asymmetric multifractal cross-correlations with crude oil, gold and DJIA as the Euro, Great British Pound and Yen. *Chaos Solitons Fractals* **2018**, *109*, 195–205. [[CrossRef](#)]
5. Yonghong, J.; He, N.; Weihua, R. Time-varying long-term memory in Bitcoin market. *Financ. Res. Lett.* **2018**, *25*, 280–284.
6. Dyhrberg, A.H. Bitcoin, gold and the dollar—a garch volatility analysis. *Financ. Res. Lett.* **2016**, *16*, 85–92. [[CrossRef](#)]
7. Dyhrberg, A.H. Hedging capabilities of bitcoin. is it the virtual gold? *Financ. Res. Lett.* **2016**, *16*, 139–144. [[CrossRef](#)]
8. Marie, B.; Kim, O.; Ariane, S. Virtual currency, tangible return: Portfolio diversification with bitcoin. *J. Asset Manag.* **2015**, *16*, 365–373.
9. Hong, K. Bitcoin as an alternative investment vehicle. *Inf. Technol. Manag.* **2017**, *18*, 265–275. [[CrossRef](#)]
10. Chuen, D.L.K.; Guo, L.; Wang, Y. Cryptocurrency: A new investment opportunity? *J. Altern. Invest.* **2017**, *20*, 16–40. [[CrossRef](#)]
11. Iwamura, M.; Kitamura, Y.; Matsumoto, T.; Saito, K. Can we stabilize the price of a Cryptocurrency?: Understanding the design of Bitcoin and its potential to compete with Central Bank money. *Hitotsub. J. Econ.* **2019**, *60*, 41–60. [[CrossRef](#)]

12. Yermack, D. Is Bitcoin a Real Currency? An Economic Appraisal. In *Handbook of Digital Currency*; Academic Press: Cambridge, MA, USA, 2015; pp. 31–44.
13. Baur, D.G.; Hong, K.H.; Lee, A.D. Bitcoin: Medium of exchange or speculative assets? *J. Int. Financ. Mark. Inst. Money* **2018**, *54*, 177–189. [[CrossRef](#)]
14. Baur, D.G.; Dimpfl, T. Asymmetric volatility in cryptocurrencies. *Econ. Lett.* **2018**, *173*, 148–151. [[CrossRef](#)]
15. Lahmiri, S.; Bekiros, S. Chaos, randomness and multi-fractality in bitcoin market. *Chaos Solitons Fractals* **2018**, *106*, 28–34. [[CrossRef](#)]
16. Lahmiri, S.; Bekiros, S.; Salvi, A. Long-range memory, distributional variation and randomness of bitcoin volatility. *Chaos Solitons Fractals* **2018**, *107*, 43–48. [[CrossRef](#)]
17. Balcihar, M.; Bouri, E.; Gupta, R.; Roubaud, D. Can volume predict Bitcoin returns and volatility? A quantiles-based approach. *Econ. Model* **2017**, *64*, 74–81. [[CrossRef](#)]
18. Katsiampa, P. Volatility estimation for bitcoin: A comparison of GARCH models. *Econ. Lett.* **2017**, *158*, 3–6. [[CrossRef](#)]
19. Chu, J.; Chan, S.; Nadarajah, S.; Osterrieder, J. GARCH modelling of cryptocurrencies. *J. Risk Financ. Manag* **2017**, *10*, 17. [[CrossRef](#)]
20. Conrad, C.; Custovic, A.; Ghysels, E. Long-and Short-Term Cryptocurrency Volatility Components: A GARCH-MIDAS Analysis. *J. Risk Financ. Manag.* **2018**, *11*, 23. [[CrossRef](#)]
21. Kristjanpoller, W.; Minutolo, M.C. A hybrid volatility forecasting framework integrating GARCH, artificial neural network, technical analysis and principal components analysis. *Expert Syst. Appl.* **2018**, *109*, 1–11. [[CrossRef](#)]
22. Peng, Y.; Albuquerque, P.H.M.; Sá, J.M.C.; Padula, A.J.A.; Montenegro, M.R. The best of two worlds: Forecasting high frequency volatility for cryptocurrencies and traditional currencies with Support Vector Regression. *Expert Syst. Appl.* **2018**, *97*, 177–192. [[CrossRef](#)]
23. Lahmiri, S.; Bekiros, S. Cryptocurrency forecasting with deep learning chaotic neural networks. *Chaos Solitons Fractals* **2019**, *118*, 35–40. [[CrossRef](#)]
24. Tseng, C.H.; Cheng, S.T.; Wang, Y.H.; Peng, J.T. Artificial neural network model of the hybrid EGARCH volatility of the Taiwan stock index option prices. *Physica A* **2008**, *387*, 3192–3200. [[CrossRef](#)]
25. Tseng, C.H.; Cheng, S.T.; Wang, Y.H. New hybrid methodology for stock volatility prediction. *Expert Syst. Appl.* **2009**, *36*, 1833–1839. [[CrossRef](#)]
26. Zahedi, J.; Rounaghi, M.M. Application of artificial neural network models and principal component analysis method in predicting stock prices on Tehran Stock Exchange. *Physica A* **2015**, *438*, 178–187. [[CrossRef](#)]
27. Kristjanpoller, W.; Minutolo, M.C. Gold price volatility: A forecasting approach using the Artificial neural network-GARCH model. *Expert Syst. Appl.* **2015**, *42*, 7245–7251. [[CrossRef](#)]
28. Kristjanpoller, W.; Minutolo, M.C. Forecasting volatility of oil price using an artificial neural network-GARCH model. *Expert Syst. Appl.* **2016**, *65*, 233–241. [[CrossRef](#)]
29. Lahmiri, S. Modeling and predicting historical volatility in exchange rate markets. *Physica A* **2017**, *471*, 387–395. [[CrossRef](#)]
30. Kristjanpoller, W.; Hernández, E. Volatility of main metals forecasted by a hybrid ANN-GARCH model with regressors. *Expert Syst. Appl.* **2017**, *84*, 290–300. [[CrossRef](#)]
31. Hajizadeh, E.; Seifi, A.; Zarandi, M.F.; Turksen, I.B. A hybrid modeling approach for forecasting the volatility of S&P 500 index return. *Expert Syst. Appl.* **2012**, *39*, 431–436.
32. Kristjanpoller, W.; Fadic, A.; Minutolo, M.C. Volatility forecast using hybrid Neural Network models. *Expert Syst. Appl.* **2014**, *41*, 2437–2442. [[CrossRef](#)]
33. Lahmiri, S.; Boukadoum, M. An ensemble system based on hybrid EGARCH-ANN with different distributional assumptions to predict S&P500 intraday volatility. *Fluct. Noise Lett.* **2015**, *14*, 1550001.
34. Seo, M.; Lee, S.; Kim, G. Forecasting the Volatility of Stock Market Index Using the Hybrid Models with Google Domestic Trends. *Fluct. Noise Lett.* **2019**, *18*, 1950006. [[CrossRef](#)]
35. Engle, R.F. Autoregressive conditional heteroscedasticity with estimates of the variance of United Kingdom inflation. *Econometrica* **1982**, *50*, 987–1007. [[CrossRef](#)]
36. Bollerslev, T. Generalized autoregressive conditional heteroskedasticity. *J. Econom.* **1986**, *31*, 307–327. [[CrossRef](#)]
37. Nelson, D.B. Conditional heteroskedasticity in asset returns: A new approach. *Econometrica* **1991**, *59*, 347–370. [[CrossRef](#)]

38. Glosten, L.; Jagannathan, R.; Runkle, D. On the relation between the expected value and the volatility nominal excess return on stocks. *J. Financ.* **1993**, *46*, 1779–1801. [[CrossRef](#)]
39. Brownlees, C.; Engle, R.; Kelly, B. A practical guide to volatility forecasting through calm and storm. *J. Risk* **2011**, *14*, 3–22. [[CrossRef](#)]
40. Giles, L.; Maxwell, T. Learning, invariance and generalization in higher order neural networks. *Appl. Opt.* **1987**, *26*, 4972–4978. [[CrossRef](#)]
41. Zhang, M.; Xu, S.; Fulcher, J. Neuron-adaptive higher order neural-network models for automated financial data modelling. *IEEE Trans. Neural Netw.* **2002**, *3*, 188–204. [[CrossRef](#)]
42. Xiong, R.; Nichols, E.P.; Shen, Y. Deep learning stock volatility with Google domestic trends. *arXiv* **2015**, arXiv:1512.04916.
43. Hamid, A.; Heiden, M. Forecasting volatility with empirical similarity and Google Trends. *J. Econ. Behav. Organ.* **2015**, *117*, 62–81. [[CrossRef](#)]
44. Dimpfl, T.; Jank, S. Can Internet search queries help to predict stock market volatility? *Eur. Financ. Manag.* **2016**, *22*, 171–192. [[CrossRef](#)]
45. Kristoufek, L. BitCoin Meets Google Trends and Wikipedia: Quantifying the Relationship between Phenomena of the Internet Era. *Sci. Rep.* **2013**, *3*, 3415. [[CrossRef](#)] [[PubMed](#)]
46. Kjærland, F.; Khazal, A.; Krogstad, E.A.; Nordstrøm, F.B.; Oust, A. An Analysis of Bitcoin's Price Dynamics. *J. Risk Financ. Manag.* **2018**, *11*, 63. [[CrossRef](#)]
47. Aalborg, H.A.; Molnár, P.; Vries, J.E. What can explain the price, volatility and trading volume of Bitcoin? *Financ. Res. Lett.* **2019**, *29*, 255–265. [[CrossRef](#)]
48. Botchkarev, A. Performance metrics (error measures) in machine learning regression, forecasting and prognostics: Properties and typology. *arXiv* **2018**, arXiv:1809.03006.
49. Kingma, D.P.; Ba, J. Adam: A method for stochastic optimization. *arXiv* **2014**, arXiv:1412.6980.
50. Hansen, P.R.; Lunde, A.; Nason, J.M. The model confidence set. *Econometrica* **2011**, *79*, 453–497. [[CrossRef](#)]



© 2020 by the authors. Licensee MDPI, Basel, Switzerland. This article is an open access article distributed under the terms and conditions of the Creative Commons Attribution (CC BY) license (<http://creativecommons.org/licenses/by/4.0/>).